The Journal of Immunology

Influenza Epitope-Specific CD8+ T Cell Avidity, but Not Cytokine Polyfunctionality, Can Be Determined by TCR^2 Clonotype

Jessica M. Moffat, Andreas Handel, Peter C. Doherty, Stephen J. Turner, Paul G. Thomas and Nicole L. La Gruta

J. Immunol. 2010;185;6850-6856; originally published online Nov 1, 2010;
doi:10.4049/jimmunol.1002025
http://www.jimmunol.org/cgi/content/full/185/11/6850

The Journal of Immunology is published twice each month by The American Association of Immunologists, Inc., 9650 Rockville Pike, Bethesda, MD 20814-3994.

Print ISSN: 0022-1767 Online ISSN: 1550-6606.

Influenza Epitope-Specific CD8$^+$ T Cell Avidity, but Not Cytokine Polyfunctionality, Can Be Determined by TCRβ Clonotype

Jessica M. Moffat,*[,1] Andreas Handel,[†] Peter C. Doherty,*[,‡] Stephen J. Turner,* Paul G. Thomas,[‡] and Nicole L. La Gruta*

Cytokine polyfunctionality has recently emerged as a correlate of effective CTL immunity to viruses and tumors. Although the determinants of polyfunctionality remain unclear, there are published instances of a link between the production of multiple effector molecules and the peptide plus MHC class I molecule avidity of T cell populations. Influenza A virus infection of C57BL/6J mice induces CTL populations specific for multiple viral epitopes, each with varying proportions of monofunctional (IFN-γ$^+$ only) or polyfunctional (IFN-γ$^+$TNF-α$^+$IL-2$^+$) CTLs. In this study, we probe the link between TCR avidity and polyfunctionality for two dominant influenza epitopes (D^bNP_{366} and D^bPA_{224}) by sequencing the TCR CDR3β regions of influenza-specific IFN-γ$^+$ versus IFN-γ$^+$IL-2$^+$ cells, or total tetramer$^+$ versus high-avidity CTLs (as defined by the peptide plus MHC class I molecule-TCR dissociation rate). Preferential selection for particular clonotypes was evident for the high-avidity D^bPA_{224}-specific set but not for any of the other subsets examined. These data suggest that factors other than TCRβ sequence influence cytokine profiles and demonstrate no link between differential avidity and polyfunctionality. ***The Journal of Immunology*****, 2010, 185: 6850–6856.**

After virus infection, CD8$^+$ T cells become activated and undergo a program of proliferation and differentiation to effector cells to facilitate viral clearance. In this capacity, a critical attribute of CD8$^+$ T cells is their ability to recognize specific peptide plus MHC class I molecule (pMHCI) complexes with sufficient avidity to induce lytic activity and the expression of effector cytokines, such as IFN-γ, TNF-α, and IL-2. Evidence suggests that distinct signaling thresholds exist for the elicitation of each of these effector functions, with cytotoxicity requiring a weaker TCR signal than is necessary for cytokine production (1, 2).

Expression of multiple effector molecules has recently emerged as a useful correlate of effective CTL immunity (3). Polyfunctional T cells have been associated with delayed disease progression after HIV infection (4–7), reduced levels of viral replication (6), and the protection afforded either by priming with vaccinia virus or vaccination against *Leishmania major* (8, 9). Greater breadth of cytokine production has also been linked to enhanced cytolytic activity in both HIV- and tumor-specific CD8$^+$ T cells (10–12). Although there have been several reports linking the functional profiles of T cell populations and their avidity or sensitivity to Ag (6, 13, 14), these analyses have been largely correlative. Furthermore, other evidence suggests that polyfunctional HIV-specific T cells partition preferentially with the set showing lower TCR avidity (15). Thus, the key determinants of polyfunctionality in virus-specific CD8$^+$ T cells, particularly the role of T cell avidity, remain unclear.

Respiratory challenge of C57BL/6 (B6) mice with influenza A viruses cause an acute, localized pneumonia that begins to resolve as virus is cleared from the lungs by day 10 postinfection (16, 17). The response characteristics after both primary and secondary influenza infection have been extensively characterized for a range of epitope-specific CD8$^+$ T cell populations (14, 18–20). In particular, cytokine production, as determined by intracellular cytokine staining, is hierarchical in character, with most of the epitope-specific CTLs producing IFN-γ, whereas some are IFN-γ$^+$TNF-α$^+$, and an even smaller subset is IFN-γ$^+$TNF-α$^+$IL-2$^+$ (14, 18). Thus, IL-2 is only produced by IFN-γ$^+$TNF-α$^+$ cells (14), and so IL-2$^+$ CTLs are referred to as "polyfunctional." Of the two dominant epitope specificities (D^bNP_{366} [influenza nucleoprotein amino acid residues 366–374 plus MHC class I H-2D^b] and D^bPA_{224} [influenza acid polymerase amino acid residues 224–232 plus MHC class I H-2D^b]), the D^bPA_{224}-specific population consistently contains significantly more polyfunctional IFN-γ$^+$TNF-α$^+$IL-2$^+$ (hereon referred to as IL-2$^+$) CD8$^+$ T cells at all phases of the response (14) and has significantly slower TCR-pMHCI dissociation rates compared with those of the D^bNP_{366}-specific population (14, 19), suggestive of a correlation between avidity and polyfunctionality in this model.

We have previously observed preferential enrichment of particular TCRβ clonotypes (defined by CDR3β amino acid sequence) in high-avidity D^bPA_{224}-specific populations, as defined by the ability to bind limiting amounts of tetramer (21). This analysis of D^bNP_{366}- and D^bPA_{224}-specific populations has now been extended by analyzing avidity based on the TCR-pMHCI

*Department of Microbiology and Immunology, University of Melbourne, Parkville, Victoria 3010, Australia; [†]Department of Epidemiology and Biostatistics, College of Public Health, University of Georgia, Athens, GA 30602; and [‡]Department of Immunology, St. Jude Children's Research Hospital, Memphis, TN 38105

[1]Current address: Immunology Division, Walter and Eliza Hall Institute of Medical Research, Parkville, Victoria, Australia.

Received for publication June 17, 2010. Accepted for publication September 29, 2010.

This work was supported by National Health and Medical Research Project Grants AI454595 (to N.L.L. and P.C.D.) and AI628316 (to N.L.L.), a National Health and Medical Research Program Grant AI567122 (to P.C.D. and S.J.T.), a National Health and Medical Research RD Wright Career Development Award (to N.L.L.), a Pfizer Australia Research Fellowship (to S.J.T.), and National Institutes of Health Grants AI70251 (to P.C.D.), AI065097, AI077714 (to P.G.T.), and AI072193 (to A.H.).

Address correspondence and reprint requests to Dr. Nicole L. La Gruta, Department of Microbiology and Immunology, University of Melbourne, Royal Parade, Parkville, VIC 3010, Australia. E-mail address: nllg@unimelb.edu.au

The online version of this article contains supplemental material.

Abbreviations used in this paper: BAL, bronchoalveolar lavage; CSA, cytokine secretion assay; ICS, intracellular cytokine staining; PI, propidium iodide; pMHCI, peptide plus MHC class I molecule.

www.jimmunol.org/cgi/doi/10.4049/jimmunol.1002025

dissociation rate, one of only two avidity measures that correlates with polyfunctionality in these populations (14, 19). Critically, we also analyzed TCRβ usage for the D^bNP_{366}- and D^bPA_{224}-specific $CD8^+$ IL-2^+ sets and compared this with TCRβ usage in the total epitope-specific IFN-γ^+ repertoires within the same mice. This allowed us to determine whether the cytokine profile of T cells after viral infection is predominantly defined by the nature of the TCR–pMHCI interaction, as evidenced by concentration of particular TCRβ clonotypes within the IL-2^+ population. Furthermore, by analyzing signatures of clonotype usage in both the high-avidity and IL-2^+ subsets, we were able to probe the relationship between CTL avidity and functionality directly.

Materials and Methods

Mice and viral infections

The female B6 (H-2^b) mice used in this study were bred and housed in the animal facility at the Department of Microbiology and Immunology, University of Melbourne (Parkville, Victoria, Australia). All experimental procedures were reviewed and approved by the University of Melbourne Animal Experimentation Ethics Committee. Naive mice (6–8 wk) were anesthetized by isoflurane inhalation and infected intranasally with 1×10^4 PFU of the A/Hong Kong x31 influenza virus (HKx31). Single-cell preparations of spleen were enriched for $CD8^+$ cells by panning for 1 h at 37˚C on plates coated with a mixture of anti-mouse IgG/IgM (Jackson ImmunoResearch Laboratories, West Grove, PA). Lymphocytes were obtained from the lung by bronchoalveolar lavage (BAL), and adherent cells were removed by incubating on plastic for 1 h at 37˚C. Four individual mice were used for each analysis of D^bNP_{366}- and D^bPA_{224}-specific TCR repertoires in total and high-avidity populations, four mice were used for the D^bPA_{224}-specific TCR repertoire analysis comparing IFN-γ^+ and IL-2^+ populations, and nine mice were used for the D^bNP_{366}-specific TCR repertoire analysis comparing IFN-γ^+ and IL-2^+ populations.

Intracellular cytokine staining

Stimulation and intracellular cytokine staining (ICS) of lymphocyte populations was performed using the BD Cytofix/Cytoperm kit (BD Biosciences, San Diego, CA) according to the manufacturer's instructions (14). Briefly, enriched BAL cells (0.5×10^6 to 1×10^6) were incubated for 5 h in 96-well round-bottom plates in 200 μl complete RPMI 1640 medium containing 1% normal mouse serum and 1 μg/ml GolgiPlug in the presence or absence of 1 μM $NP_{366–374}$ (ASNENMETM) or $PA_{224–233}$ (SSLENFRAYV) peptides (Auspep, Tullamarine, Australia). Cells were then stained with anti-CD8α–PerCP–Cy5.5 Ab (BD Biosciences), fixed, permeabilized, and stained with anti–IFN-γ–FITC and anti–IL-2–PE Abs (BioLegend, San Diego, CA). Data were acquired on an LSRII Benchtop Analyzer (BD Immunocytometry Systems, San Jose, CA) and analyzed using CellQuest Pro Software (BD Immunocytometry Systems).

Cytokine secretion assay

Stimulation and cell surface cytokine staining of lymphocyte populations was performed using the cytokine secretion assay (CSA; Miltenyi Biotec, North Ryde, NSW, Australia) according to the manufacturer's instructions. Briefly, enriched BAL cells were stimulated in vitro for 5 h in the presence or absence of 1 μM NP_{366} or PA_{224} peptide. Cells were washed with secretion assay buffer (PBS containing 10% BSA plus 2 mM EDTA, pH 8), and stained with IFN-γ and IL-2 catch reagents (Miltenyi Biotec). Samples were incubated at 37˚C for 45 min under continuous rotation to allow cytokine secretion to occur, after which they were stained with anti–IFN-γ–PE, anti–IL-2–allophycocyanin detection Abs, and anti-CD8α–PerCP–Cy5.5 (BD Biosciences) (22). Propidium iodide (PI; 0.5 μg/ml) was added prior to sample acquisition on an LSRII Benchtop Analyzer or cell sorting using a FACSAria Cell Sorter (BD Immunocytometry Systems). For sorting experiments, individual $CD8^+$IFN-γ^+PI^- or $CD8^+$IFN-γ^+IL-2^+PI^- cells were sorted into the wells of a 96-well PCR plate. Data were analyzed using CellQuest Pro Software.

Tetramer dissociation

Enriched splenocytes (0.1×10^6 to 2×10^6 cells) were stained with D^bNP_{366}–PE or D^bPA_{224}–PE tetramers for 1 h at room temperature. The cells were then incubated for various times at 37˚C in buffer containing 50 μg/ml anti–H-$2D^b/K^b$ Ab (28-8-6; BD Biosciences) to prevent tetramer rebinding. Cells were then washed and stained with anti-CD8α–PerCP–Cy5.5 and either anti-Vβ8.3–FITC (TRBV13-1) (D^bNP_{366}) or anti-Vβ7–FITC (TRBV29) (D^bPA_{224}) (BD Biosciences), washed, and analyzed (19). Individual $CD8^+D^bNP_{366}^+V\beta8.3^+$ or $CD8^+D^bPA_{224}^+V\beta7^+$cells cells were sorted, either prior to anti–H-$2D^b/K^b$ Ab incubation (T0) or after 60 min incubation (T60), into wells of a 96-well plate using a FACSAria Cell Sorter (BD Immunocytometry Systems).

Single-cell analysis of TCR

Reverse transcription was performed on individual sorted cells as described previously, and a nested PCR strategy was used to amplify Vβ8.3 (D^bNP_{366}) or Vβ7 (D^bPA_{224}) cDNA using published external and internal oligonucleotide primers (23–25). Second-round Vβ PCR products (2–3 μl) were then purified using the Qiaquick PCR Purification Kit (Qiagen, Hilden, Germany), sequenced using 3.2 pmol of the internal Vβ primer, and analyzed on an ABI Prism 3700 sequence analyzer.

Statistical analyses

Unless otherwise stated, analysis of statistical significance was determined using a paired Student *t* test, with a *p* value of 0.05 used to define significance. A Fisher's exact test was used to determine significance in Fig. 3, with *p* values combined using Stouffer's method. The Morisita-Horn similarity index was used to probe the similarity between the total epitope-specific TCRβ repertoire and either the high-avidity or IL-2–producing subsets (26).

Results

Identification of high-avidity cells by tetramer dissociation

The tetramer dissociation assay provides a relative measure of the duration of the TCR–pMHCI interaction for polyclonal epitope-specific T cell populations (14, 19, 27). Relative rates of TCR dissociation for D^bNP_{366}- and D^bPA_{224}-specific populations were shown previously to correlate with the respective proportions of polyfunctional CTLs in these populations (14, 19). To determine whether the signatures of TCRβ clonotype usage in high-avidity D^bNP_{366} and D^bPA_{224}-specific CTL populations was similar to that observed previously using limiting amounts of tetramer, tetramer dissociation was performed on splenocytes from mice infected intranasally with HKx31 10 d previously (Fig. 1). Analysis of D^bNP_{366} or D^bPA_{224} tetramer dissociation was limited to those cells expressing the dominant Vβ gene [TRBV13-1 or TRBV29, respectively (28, 29)]. Total $tetramer^+$ cells were isolated prior to addition of the anti–H-$2D^b/K^b$ Ab (Fig. 1*B*, 1*D*; 0 min), and high-avidity cells were classified as those remaining tetramer-bound after a 60-min incubation with the anti–H-$2D^b/K^b$ Ab (Fig. 1*B*, 1*D*; 60 min). For both the D^bNP_{366}- and D^bPA_{224}-specific sets, the population isolated at 60 min represented between 13 and 20% of the maximum staining observed at time 0 (Fig. 1*A*, 1*C*).

Identification of IFN-γ^+ and IFN-γ^+IL-2^+ cells by CSA

Using the ICS assay (14, 18, 24), we have previously demonstrated that the production of cytokines by influenza virus-specific $CD8^+$ T cells postinfection is hierarchical. Thus, whereas the vast majority of influenza-specific CTLs make IFN-γ after short-term in vitro restimulation, only a small subset of these cells also produces IL-2. The CSA used in the current study measures secreted cytokine that is retained on the surface of previously activated cells, allowing the specific isolation of viable cells based on their cytokine production profiles (22). This avoids the limitation of the ICS assay, which has a requisite fixation step that hinders any subsequent analysis of gene expression due to the damaging effects of formalin on nucleic acids (30). To determine whether the hierarchical nature of cytokine production observed routinely using ICS is also found by CSA, we harvested BAL cells from mice infected 10 d earlier and used both techniques to assay for IFN-γ and IL-2 production after short-term in vitro restimulation with the NP_{366} peptide (Fig. 2*A*). Generally, the sensitivity of the CSA was slightly reduced compared with that of ICS, resulting in the

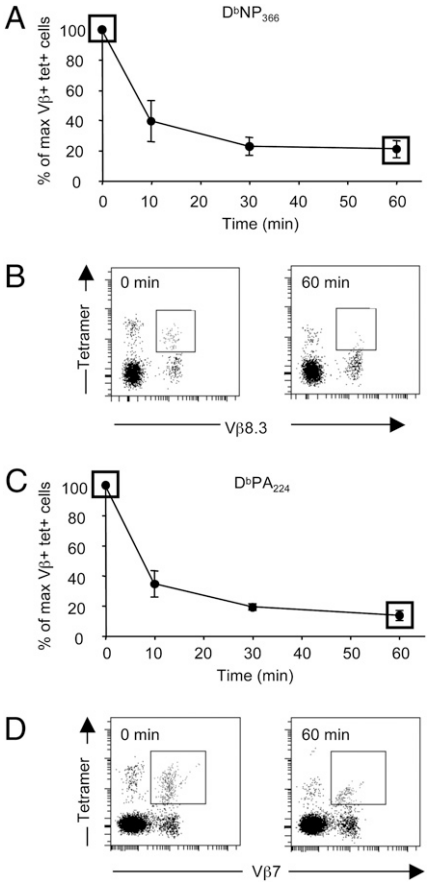

FIGURE 1. Tetramer dissociation and isolation of high-avidity CTLs. Splenocytes from mice infected with influenza virus intranasally 10 d previously were bound with D^bNP_{366} or D^bPA_{224} tetramer then incubated in the presence of anti–H-$2D^b/K^b$ (28-8-6) Ab for designated times. Cells were then stained with anti-CD8α–FITC and either anti-Vβ8.3–PE (TRBV13-1; D^bNP_{366}) or anti-Vβ7–PE (TRBV29; D^bPA_{224}). Shown are $CD8^+$ $tetramer^+$ $TRBV^+$ cells expressed as the mean percentage ± SD of the maximum population observed at time 0 (*A*, *C*) ($n = 4$ mice per group). Representative dot plots show Vβ and tetramer staining of $CD8^+$ T cells at 0 min (total tetramer+) and 60 min (high avidity), at which times cells were isolated using the gates shown (*B*, *D*). Data are representative of at least three independent experiments.

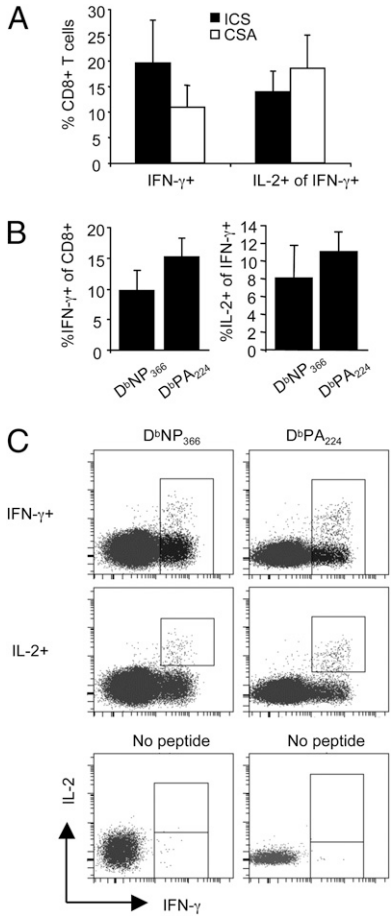

FIGURE 2. Characterization and isolation of differential cytokine-producing CTLs by CSA. Cells isolated from the BAL of mice infected intranasally with influenza A virus 10 d previously were stimulated in vitro with NP_{366} peptide for 5 h, and cytokine production was identified by ICS or CSA. *A*, Shown is the percentage ± SD of $CD8^+$ T cells that were IFN-γ^+ and the proportion of those cells that were IL-2^+ by each technique ($n = 5$ mice per group). Data reflect CSA on day-10-infected BAL cells stimulated with NP_{366} or PA_{224} peptide. *B*, Shown is the percentage ± SD of $CD8^+$ T cells that are IFN-γ^+ and the proportion of those cells that are IL-2^+ ($n = 4$ mice per group). *C*, Representative dot plots showing IFN-γ and IL-2 staining on $CD8^+$ T cells using CSA. The gates used to isolate the two cell populations are shown. For all quantitation of epitope-specific responses, values from no peptide controls have been subtracted. Data are representative of at least three independent experiments.

detection of fewer IFN-γ^+ cells after in vitro restimulation (Fig. 2*A*). Despite this, the relative cytokine hierarchy was maintained (Fig. 2*C*), and the proportion of IFN-γ^+ cells that also produced IL-2 was similar for the two techniques (Fig. 2*A*). Furthermore, both the magnitude and the proportion of $CD8^+$IFN-γ^+ cells producing IL-2 was slightly (although not significantly) larger for the D^bPA_{224}-specific set compared with that of the D^bNP_{366}-specific population (Fig. 2*B*), replicating previous ICS findings for acute-stage BAL cells (31).

CDR3β length and Jβ usage within high-avidity and IL-2–producing CTL subsets

Analysis of CDR3β lengths and Jβ usage in either the total IFN-γ^+ or $tetramer^+$ populations (Supplemental Tables I–IV) confirmed the previously identified biases of 9 aa and TRBJ2S2 usage for D^bNP_{366}-specific populations, and 6–7 aa and TRBJ1S1 and 2S6 usage for D^bPA_{224}-specific $CD8^+$ T cell populations (Fig. 3, $tetramer^+$ and IFN-γ^+ columns) (23, 25).

For the high-avidity D^bNP_{366}-specific subset, CDR3β length and Jβ distributions paralleled the total $tetramer^+$ $CD8^+$ set (Fig. 3*A*, 3*B*). By contrast, the high-avidity D^bPA_{224}-specific population showed a significant divergence from its corresponding total $tetramer^+$ set ($p < 0.0001$). The contribution of clonotypes (i.e., unique TCRβ sequences) expressing a CDR3β length of 6 aa decreased from 74% of the total $D^bPA_{224}{}^+$ cells to 44% for the high-avidity subset, with a corresponding increase in clonotypes with a CDR3β length of 7 aa (18–39%) (Fig. 3*A*). Scrutiny of the TCR CDR3β amino acid sequence data established that this increase correlated with a substantial increase in the prevalence of clonotypes with a 7-aa CDR3β length in three of the four mice analyzed, with the fourth mouse showing a substantial overrepresentation of an 11-aa length clonotype (Supplemental Table II). A less pronounced but still significant difference ($p < 0.005$) was also observed for Jβ usage between the total and high-avidity D^bPA_{224}-specific populations (Fig. 3*B*).

Notably, analysis of the D^bNP_{366}- and D^bPA_{224}-specific IL-2^+ subsets showed profiles that were very similar to the respective IFN-γ^+ populations, both with respect to CDR3β length and Jβ

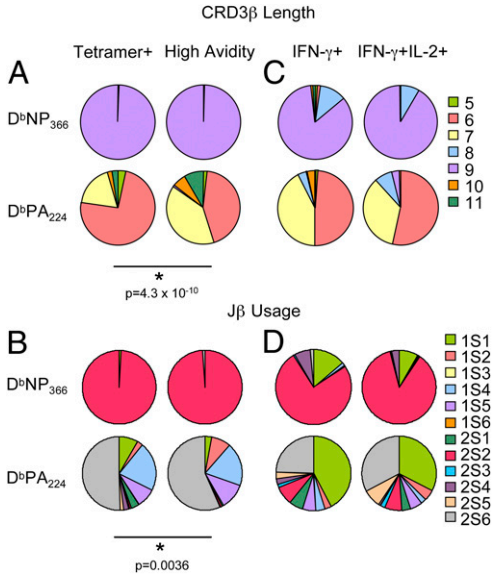

FIGURE 3. TCR CDR3β length and Jβ usage within high-avidity and IL-2$^+$ subsets. Usage of particular CDR3β lengths (*A*, *C*) and Jβ gene elements (*B*, *D*) was determined from CDR3β sequences obtained by single-cell RT-PCR of D^{b}NP$_{366}$ or D^{b}PA$_{224}$-specific CD8$^+$ T cells isolated based on tetramer binding (*A*, *B*) or on cytokine production (*C*, *D*). Data are summarized in pie charts where each slice of the pie represents the proportion of sequences from each sample group (D^{b}NP$_{366}$-specific: total tetramer$^+$ n = 232, high-avidity n = 202, total IFN-γ$^+$ n = 203, IL-2$^+$ n = 159; D^{b}PA$_{224}$-specific: total tetramer$^+$ n = 166, high-avidity n = 106, total IFN-γ$^+$ n = 225, IL-2$^+$ n = 149) using a particular CDR3β length (*A*, *C*) or Jβ region (*B*, *D*). *Significance determined using Fisher's exact test on individual mice, with the p values combined using Stouffer's method.

usage (Fig. 3*C*, 3*D*). There was, in fact, no evidence that differential cytokine production profiles reflected any pattern of TCR repertoire selection for either D^{b}NP$_{366}$ or D^{b}PA$_{224}$, a situation that was quite different from the total versus high-avidity D^{b}PA$_{224}$-specific populations. Thus, at this broad level of analysis, the polyfunctional IL-2–producing subset of virus-specific CD8$^+$ T cells does not appear to be using a characteristically distinct subset of TCRs, nor is there any obvious parallel with the selective clonotype usage that characterizes the high-avidity D^{b}PA$_{224}$-specific set.

Dominant clonotypes in high-avidity and IL-2$^+$ populations

If, given sufficient TCR-pMHCI avidity to achieve tetramer binding or trigger IFN-γ production, the TCR contributes significantly to differential CTL avidity and/or function in mice, one might expect to see enrichment of particular TCRβ clonotypes in the high-avidity or polyfunctional IL-2$^+$ subsets, respectively. Clonotypes from the four sample groups were arbitrarily divided into those that contributed to ≤10% (minor), 11–40% (intermediate), or ≥41% (dominant) of the total repertoire analyzed within individual mice and were plotted as a proportion of the total clonotypes (Fig. 4*A*–*D*). As expected, analysis of the total tetramer$^+$ or IFN-γ$^+$ D^{b}PA$_{224}$-specific cells confirmed that they were predominantly composed of minor clonotypes, with virtually no dominant species evident (Fig. 4*A*, 4*C*, closed circles) (23). In contrast, the total tetramer$^+$ or IFN-γ$^+$ D^{b}NP$_{366}$-specific sets showed a greater contribution of intermediate and dominant clonotypes (Fig. 4*B*, 4*D*, closed circles). These D^{b}NP$_{366}$-specific populations were also more variable between mice, reflecting the smaller number of large clonotypes identified. As a consequence, those that were found represented a larger percentage of the total.

Intriguingly, analysis of CDR3β profiles in the high-avidity populations showed a significant increase (p = 0.008) in the proportion of dominant (≥41%) D^{b}PA$_{224}$-specific clonotypes, from zero in the total tetramer$^+$ population to between 11 and 25% for the four mice analyzed (Fig. 4*A*, open circles). Similar trends of preferential TCRβ usage were found when the classification of "dominant clonotypes" was altered to ≥20% (p = 0.004) or ≥30% (p = 0.11), confirming that there is no bias associated with this arbitrary categorization. In contrast, there was no evidence of clonotype enrichment in the high-avidity D^{b}NP$_{366}$ subset relative to the total population (p = 0.55) (Fig. 4*B*, open circles).

Performing the same analysis for the IL-2$^+$ subset versus the total IFN-γ$^+$ CTLs, no enrichment was evident for dominant clonotypes in the D^{b}PA$_{224}$-specific set, with both populations of cytokine-producing cells showing strikingly similar profiles (Fig. 4*C*). Thus, unlike the situation for the high-avidity D^{b}PA$_{224}$-specific population, there was no evidence of selective TCRβ usage in the IL-2$^+$ set (Fig. 4*A* compared with 4*C*). Furthermore, no significant differences in clonotype distribution were found for the IFN-γ$^+$ and IL-2$^+$ D^{b}NP$_{366}$-specific sets (Fig. 4*D*), suggesting that neither differential avidity nor function within the D^{b}NP$_{366}$-specific population is primarily determined by CDR3β clonotype.

The analyses thus far identified, among other parameters, the relative contribution of dominant clonotypes to each population. We next assessed whether the particular clonotypes that were dominant within the high-avidity or IL-2$^+$ subsets were selectively enriched from the total epitope-specific population. To this end, we determined the frequency of the single most dominant clonotype within either the high-avidity or IL-2$^+$ subsets from each mouse and analyzed the corresponding frequency of these clonotypes within the total tetramer$^+$ and IFN-γ$^+$ populations, respectively (Fig. 4*E*). In support of our earlier analysis (Fig. 4*A*–*D*), we found that a selectively greater prevalence of the dominant clonotype was characteristic only of the high-avidity D^{b}PA$_{224}$-specific population. In contrast, neither the dominant clonotypes in the high-avidity D^{b}NP$_{366}$-specific population nor those in the IL-2$^+$ subsets showed any significant enrichment over the frequency in the total epitope-specific populations (Fig. 4*E*), suggesting that these clonotypes play no part in determining differential function or avidity.

Clonotype sharing in high-avidity D^{b}PA$_{224}$-specific populations

If the same clonotype(s) were responsible for conferring enhanced D^{b}PA$_{224}$-specific TCR avidity in all four of the individuals analyzed, we might expect the degree of repertoire "sharing" (i.e., the proportion of an individual's repertoire that is found in ≥50% of mice analyzed) to be selectively increased in the high-avidity set. The proportion of each total epitope-specific CTL response (based on tetramer staining or IFN-γ production) that was "shared" was found to be significantly lower in the D^{b}PA$_{224}$-specific compared with the D^{b}NP$_{366}$-specific populations, which is consistent with previous characterizations of these repertoires as "private" and "public," respectively (23, 25) (D^{b}NP$_{366}$, 84 ± 14% [derived from 11 primary immune mice and 723 sequences]; D^{b}PA$_{224}$, 13 ± 6.8% [derived from 13 primary immune mice and 759 sequences]) (Fig. 5). Notably, despite clear evidence of clonotype enrichment in the high-avidity D^{b}PA$_{224}$-specific populations for all four mice analyzed (Fig. 4*A*, 4*E*), the proportion of the response that was shared in this subset was similar to the total tetramer$^+$ population. These data establish, therefore, that the same clonotype(s) are not responsible for conferring a high-avidity TCR phenotype in all mice. This is confirmed by looking directly at the CDR3β amino acid sequences; of the five clonotypes identified as dominant in high-avidity D^{b}PA$_{224}$-specific populations, only one (SLGGYEQ) was dominant in

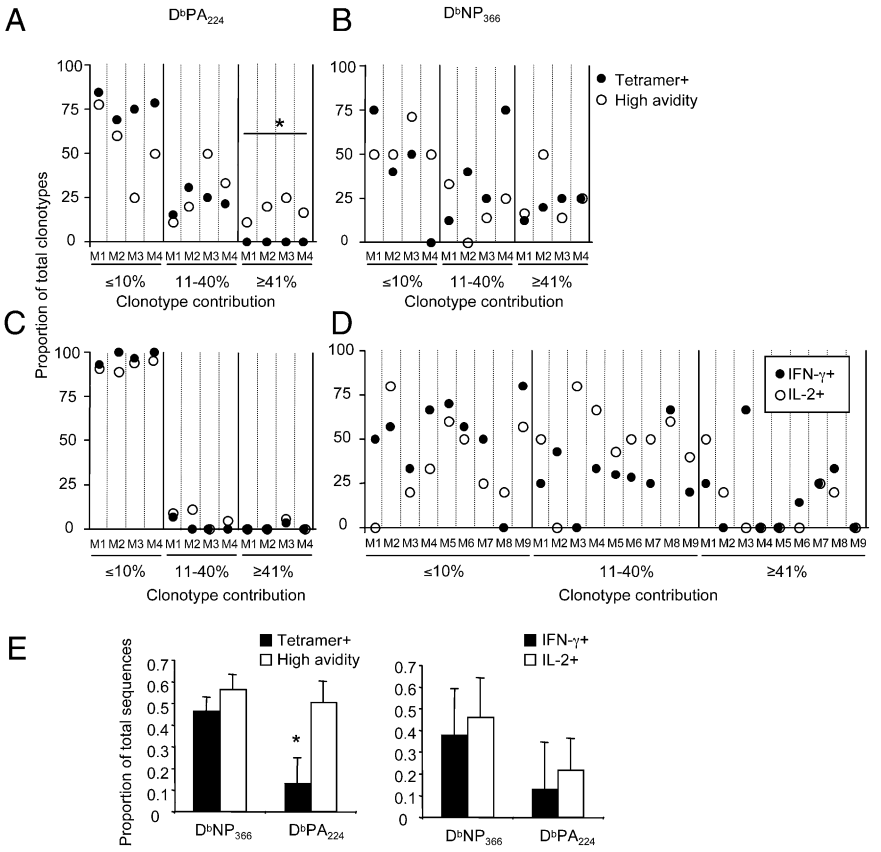

FIGURE 4. CDR3β clonotype size in high-avidity and IL-2$^+$ CTL populations. CDR3β clonotypes identified from total tetramer$^+$ or high-avidity populations (*A*, *B*) or IFN-γ$^+$ or IL-2$^+$ populations (*C*, *D*) were divided based on their contribution to the total sequenced repertoire within each of the four groups (see legend to Fig. 3 for number of sequences analyzed). The prevalence of clonotypes within each of these categories was then plotted as a percentage of all CDR3β clonotypes observed within each group. Data from each mouse are plotted individually. Comparison of total epitope-specific to high-avidity or IL-2$^+$ subsets using a Student paired *t* test: $*p < 0.01$ (*A–D*). For each mouse, the frequency of the single most dominant clonotype within either the high-avidity or IL-2$^+$ subsets was determined for the total tetramer$^+$ and IFN-γ$^+$ populations, respectively (*E*). $*p < 0.005$ using a Student paired *t* test.

more than one individual (Supplemental Table II). Thus it appears that, within the typically diverse D^{b}PA$_{224}$-specific TCRβ repertoire, there are a number of clonotypes that can confer a high-avidity phenotype.

Similarity of total and subset TCRβ repertoires

We have compared clonotype abundance and sharing between the total and the subsets of epitope-specific CTL populations and have shown a significant difference only for the high-avidity D^{b}PA$_{224}$-specific population. To analyze the populations in more detail, the similarity of total epitope-specific repertoires and the subsets of repertoires was compared within individual mice using the Morisita-Horn similarity index (26) (Fig. 6). The Morisita-Horn index accounts for both the number of common clonotypes and the distribution of clone sizes, giving a value of 1 for clonotype groups that are identical and a value of zero for completely distinct groups. Reference pairs were generated by randomly distributing (10,000 times) pooled clonotypes from individual mice (i.e., taken from both the total epitope-specific population and the subset) into groups of the same size. The reference pairs, showing the similarity of randomized groups (Fig. 6, white bars), are then compared with the actual pairs, showing the similarity of the total versus the subset groups found within individual mice (black bars). In all cases, the reference pairs were slightly more similar than was observed for the actual pairs, which is possibly a consequence of individual differences [e.g., mice 3 and 5 (Supplemental Table III)] or minor sampling discrepancies. Again, despite these subtle differences, the only subset that was significantly dissimilar from the total population was the high-avidity D^{b}PA$_{224}$-specific subset ($p = 0.008$), suggesting distinct clonotype usage within this subset compared with that of the total population.

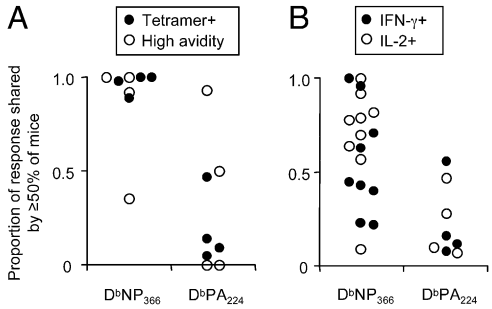

FIGURE 5. CDR3β clonotype sharing in high-avidity and IL-2$^+$ CTL populations. The proportion of the CTL response (based on CDR3β sequences) that was "shared" between individuals (found in ≥50% of mice analyzed) is shown for the total tetramer$^+$ and high-avidity populations (*A*) or IFN-γ$^+$ and IL-2$^+$ populations (*B*).

Discussion

The avidity of the TCR–pMHCI interaction has long been considered to heavily influence the efficiency with which CD8$^+$ T cells respond to viral infections (32–35) and tumors (36–38). Similarly, the capacity of T cells to produce multiple effector cytokines has also emerged as a positive correlate of effective CTL immunity (4–9, 11, 12). Furthermore, those studies that investigated the link between these characteristics suggested that it was the high-avidity T cell populations that tend to exhibit cytokine polyfunctionality (6, 7). In this study, we investigated the involvement of TCRβ clonotype in determining avidity and polyfunctional phenotype for two influenza virus-specific CTL populations. To our knowledge, this represents the first analysis of TCR repertoires associated with differential CTL effector function.

We found that TCRβ clonotype appeared to influence differential TCR-pMHCI avidity only within the D^{b}PA$_{224}$-specific CTL

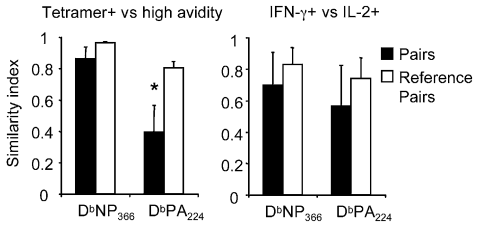

FIGURE 6. Similarity comparison between total and subsets of epitope-specific populations using Morisita-Horn similarity index. The Morisita-Horn similarity index (26) was used to compare the similarity of the total epitope-specific population (either tetramer$^+$ or IFN-γ^+) with the corresponding subset (either high avidity or IL-2$^+$). The value obtained for each pair of samples was compared with a value generated by random distribution (10,000 times) of the pooled clonotypes into groups of the same size (reference pairs). Shown are the mean similarity values ± SD of actual and reference pairs for each sample group analyzed.

sets, whereas polyfunctional IL-2$^+$ cells showed no preferential usage of particular TCRβs in either the D^bNP_{366}- or D^bPA_{224}-specific CTL populations. Therefore, at least in the case of the D^bPA_{224}-specific set, there is no obvious link between TCR avidity and polyfunctionality.

The observation that only the high-avidity D^bPA_{224}-specific subset showed any substantial divergence from the total epitope-specific population supports data published previously, in which total and high-avidity D^bNP_{366}- and D^bPA_{224}-specific CD8$^+$ T cell populations were segregated using tetramer dilution rather than tetramer dissociation (21). In that study, the selective enrichment of TCRβ clonotypes in the D^bPA_{224}-specific, but not the D^bNP_{366}-specific, high-avidity population was interpreted as a reflection that the more diverse (by CDR3β clonotype) D^bPA_{224}-specific repertoire encoded a broader range of avidities compared with that of the more restricted D^bNP_{366}-specific repertoire, thus facilitating the observation of TCRβ partitioning within this population. Data have recently emerged, however, that TCRα-chain usage in the TCRβ-"restricted" D^bNP_{366}-specific population is more varied than the TCRα profiles for the TCRβ-"diverse" D^bPA_{224}-specific set (Day et al., unpublished data). Taking this into account, it is possible that the D^bNP_{366}- and D^bPA_{224}-specific CTL populations have comparable numbers of TCRαβ clonotypes (and thus range of avidities), but differential partitioning of clonotypes may only become evident when the more variable chain is analyzed (whether α or β). Although the restriction of our analyses to the contribution of TCRβ-chain to differential avidity and polyfunctionality precludes any comment on the contribution of the TCRα-chain, the current analysis does allow us to state definitively that distinct CTL populations are responsible for conferring avidity and polyfunctional phenotypes in the D^bPA_{224}-specific population.

One might have anticipated differences between the previous analysis of avidity based on the sensitivity of TCR-pMHCI binding (which takes into account both the on- and off-rates of binding) and the current analysis that is based on the TCR-pMHCI dissociation rate, a measure that has been shown previously to correlate with different levels of polyfunctionality for D^bNP_{366}- and D^bPA_{224}-specific populations (14, 19). The fact that these two strategies for subsetting high-avidity cells yielded a similar difference (selectively in the D^bPA_{224}-specific subset), and enrichment of the same TCRβ clonotype (SLGGYEQ) in some mice, suggests that the contribution of TCRβ clonotype to avidity that was detected in the earlier study (21) was dictated primarily by the effects on dissociation rate and not the on-rate of binding.

Previous studies have shown that clonal T cell populations, such as TCR transgenic cells, show a spectrum of cytokine production profiles, indicating that polyfunctionality in T cells cannot be solely defined by TCR clonotype (31, 39). However, it remained possible that, in a polyclonal population, TCR clonotype could be a determinant of broad-spectrum cytokine production. However, the current analysis provides no evidence of a correlation between TCRβ sequence and cytokine polyfunctionality, suggesting that TCRβ clonotype neither dictates nor influences this CTL function. This was particularly intriguing for the D^bPA_{224}-specific population, where we saw clear partitioning of clonotypes in the high-avidity subset, and suggests that polyfunctionality (at least for this epitope) is not a selective characteristic of the high-avidity population. This is supported by one study (15) in which polyfunctionality correlated more closely with the HLA restriction element and was inversely correlated with avidity, but contrasts with a number of other studies (including our own) that have indicated a link between the strength of the TCR–pMHCI interaction and the propensity to produce multiple cytokines (6, 7, 13, 14, 19). Critically, however, the nexus between avidity and polyfunctionality in the majority of these studies was correlative, leaving open the possibility that these two effects segregate independently. Further evidence that cytokine profiles are determined independently of TCR avidity comes from our earlier observation that the threshold of stimulation required for the production of IFN-γ, TNF-α, and IL-2 in influenza epitope-specific CTL populations is equivalent. That is, polyfunctional epitope-specific CTLs were found at comparable prevalence when cells were stimulated with optimal or suboptimal peptide concentrations and in CD8-dependent and -independent responses (19). Although some apparent differences in clonotype usage were observed in the current study between the D^bNP_{366}-specific IFN-γ versus IL-2 groups for particular mice [i.e., notably mice 3 and 5 (Supplemental Table III)], such differences were not generally characteristic of these groups, and the total analysis of all nine mice in this group did not support the contention that TCRβ clonotype is able to confer polyfunctionality at the global level.

If TCR-pMHCI avidity, beyond the minimal level to induce functional activity, plays little part in tuning the level of cytokine induction, what are the critical determinants of this effector function? Multiple studies have recently indicated that inflammatory signals have a substantial influence on the differentiation of CD8$^+$ T cells into effector and/or memory CTLs. Notably, it seems that inflammation can promote the acquisition of CTL effector functions (including IFN-γ and granzyme B expression) and delay the progression into memory (40, 41). Recent evidence suggests that the path to an effector or memory phenotype is further regulated by a complex interplay between both inflammatory and IL-2 signals (42, 43). Relating these findings to our model of influenza virus infection, we routinely observe a significantly larger proportion of polyfunctional virus-specific CTLs at the site of infection (BAL) compared with that of the spleen at the acute stage of primary infection (14, 18). Thus, it is likely that these site-related differences in cytokine profiles reflect that the inflammatory environment of the infected lung selectively promotes the full acquisition and retention of CTL effector functions.

Taken together, our data demonstrate a clear role for TCRβ clonotype in determining the TCR avidity of one (but not another) influenza-specific CTL population, thus highlighting the differential contribution of the TCRβ-chain to pMHCI recognition mediated by diverse epitope-specific TCRs. Furthermore, our data suggest that after influenza virus infection, polyfunctional CTLs are not necessarily contained within the high-avidity population. These data suggest that a focus on the cytokine/chemokine milieu during priming rather than an emphasis on maximizing TCR-pMHCI avidity may be a better strategy for optimizing vaccine efficacy.

Acknowledgments

We thank Dr. Katherine Kedzierska and Dr. Matthew Olson for critical review of the manuscript.

Disclosures

The authors have no financial conflicts of interest.

References

1. Faroudi, M., C. Utzny, M. Salio, V. Cerundolo, M. Guiraud, S. Müller, and S. Valitutti. 2003. Lytic versus stimulatory synapse in cytotoxic T lymphocyte/target cell interaction: manifestation of a dual activation threshold. *Proc. Natl. Acad. Sci. USA* 100: 14145–14150.
2. Valitutti, S., S. Müller, M. Dessing, and A. Lanzavecchia. 1996. Different responses are elicited in cytotoxic T lymphocytes by different levels of T cell receptor occupancy. *J. Exp. Med.* 183: 1917–1921.
3. Seder, R. A., P. A. Darrah, and M. Roederer. 2008. T-cell quality in memory and protection: implications for vaccine design. *Nat. Rev. Immunol.* 8: 247–258.
4. Betts, M. R., M. C. Nason, S. M. West, S. C. De Rosa, S. A. Migueles, J. Abraham, M. M. Lederman, J. M. Benito, P. A. Goepfert, M. Connors, et al. 2006. HIV nonprogressors preferentially maintain highly functional HIV-specific CD8+ T cells. *Blood* 107: 4781–4789.
5. Duvall, M. G., M. L. Precopio, D. A. Ambrozak, A. Jaye, A. J. McMichael, H. C. Whittle, M. Roederer, S. L. Rowland-Jones, and R. A. Koup. 2008. Polyfunctional T cell responses are a hallmark of HIV-2 infection. *Eur. J. Immunol.* 38: 350–363.
6. Almeida, J. R., D. A. Price, L. Papagno, Z. A. Arkoub, D. Sauce, E. Bornstein, T. E. Asher, A. Samri, A. Schnuriger, I. Theodorou, et al. 2007. Superior control of HIV-1 replication by CD8+ T cells is reflected by their avidity, polyfunctionality, and clonal turnover. *J. Exp. Med.* 204: 2473–2485.
7. Almeida, J. R., D. Sauce, D. A. Price, L. Papagno, S. Y. Shin, A. Moris, M. Larsen, G. Pancino, D. C. Douek, B. Autran, et al. 2009. Antigen sensitivity is a major determinant of CD8+ T-cell polyfunctionality and HIV-suppressive activity. *Blood* 113: 6351–6360.
8. Precopio, M. L., M. R. Betts, J. Parrino, D. A. Price, E. Gostick, D. R. Ambrozak, T. E. Asher, D. C. Douek, A. Harari, G. Pantaleo, et al. 2007. Immunization with vaccinia virus induces polyfunctional and phenotypically distinctive CD8(+) T cell responses. *J. Exp. Med.* 204: 1405–1416.
9. Darrah, P. A., D. T. Patel, P. M. De Luca, R. W. Lindsay, D. F. Davey, B. J. Flynn, S. T. Hoff, P. Andersen, S. G. Reed, S. L. Morris, et al. 2007. Multifunctional TH1 cells define a correlate of vaccine-mediated protection against *Leishmania major*. *Nat. Med.* 13: 843–850.
10. Imai, N., H. Ikeda, I. Tawara, and H. Shiku. 2009. Tumor progression inhibits the induction of multifunctionality in adoptively transferred tumor-specific CD8+ T cells. *Eur. J. Immunol.* 39: 241–253.
11. Rizzuto, G. A., T. Merghoub, D. Hirschhorn-Cymerman, C. Liu, A. M. Lesokhin, D. Sahawneh, H. Zhong, K. S. Panageas, M. A. Perales, G. Altan-Bonnet, et al. 2009. Self-antigen-specific CD8+ T cell precursor frequency determines the quality of the antitumor immune response. *J. Exp. Med.* 206: 849–866.
12. Lichterfeld, M., X. G. Yu, M. T. Waring, S. K. Mui, M. N. Johnston, D. Cohen, M. M. Addo, J. Zaunders, G. Alter, E. Pae, et al. 2004. HIV-1-specific cytotoxicity is preferentially mediated by a subset of CD8(+) T cells producing both interferon-gamma and tumor necrosis factor-alpha. *Blood* 104: 487–494.
13. Aagaard, C., T. T. Hoang, A. Izzo, R. Billeskov, J. Troudt, K. Arnett, A. Keyser, T. Elvang, P. Andersen, and J. Dietrich. 2009. Protection and polyfunctional T cells induced by Ag85B-TB10.4/IC31 against Mycobacterium tuberculosis is highly dependent on the antigen dose. *PLoS One* 4: e5930.
14. La Gruta, N. L., S. J. Turner, and P. C. Doherty. 2004. Hierarchies in cytokine expression profiles for acute and resolving influenza virus-specific CD8+ T cell responses: correlation of cytokine profile and TCR avidity. *J. Immunol.* 172: 5553–5560.
15. Harari, A., C. Cellerai, F. B. Enders, J. Köstler, L. Codarri, G. Tapia, O. Boyman, E. Castro, S. Gaudieri, I. James, et al. 2007. Skewed association of polyfunctional antigen-specific CD8 T cell populations with HLA-B genotype. *Proc. Natl. Acad. Sci. USA* 104: 16233–16238.
16. Doherty, P. C., and J. P. Christensen. 2000. Accessing complexity: the dynamics of virus-specific T cell responses. *Annu. Rev. Immunol.* 18: 561–592.
17. Allan, W., Z. Tabi, A. Cleary, and P. C. Doherty. 1990. Cellular events in the lymph node and lung of mice with influenza. Consequences of depleting CD4+ T cells. *J. Immunol.* 144: 3980–3986.
18. Belz, G. T., W. Xie, and P. C. Doherty. 2001. Diversity of epitope and cytokine profiles for primary and secondary influenza a virus-specific CD8+ T cell responses. *J. Immunol.* 166: 4627–4633.
19. La Gruta, N. L., P. C. Doherty, and S. J. Turner. 2006. A correlation between function and selected measures of T cell avidity in influenza virus-specific CD8+ T cell responses. *Eur. J. Immunol.* 36: 2951–2959.
20. Flynn, K. J., G. T. Belz, J. D. Altman, R. Ahmed, D. L. Woodland, and P. C. Doherty. 1998. Virus-specific CD8+ T cells in primary and secondary influenza pneumonia. *Immunity* 8: 683–691.
21. Kedzierska, K., N. L. La Gruta, M. P. Davenport, S. J. Turner, and P. C. Doherty. 2005. Contribution of T cell receptor affinity to overall avidity for virus-specific CD8+ T cell responses. *Proc. Natl. Acad. Sci. USA* 102: 11432–11437.
22. Campbell, J. D. 2003. Detection and enrichment of antigen-specific CD4+ and CD8+ T cells based on cytokine secretion. *Methods* 31: 150–159.
23. Kedzierska, K., S. J. Turner, and P. C. Doherty. 2004. Conserved T cell receptor usage in primary and recall responses to an immunodominant influenza virus nucleoprotein epitope. *Proc. Natl. Acad. Sci. USA* 101: 4942–4947.
24. La Gruta, N. L., P. G. Thomas, A. I. Webb, M. A. Dunstone, T. Cukalac, P. C. Doherty, A. W. Purcell, J. Rossjohn, and S. J. Turner. 2008. Epitope-specific TCRbeta repertoire diversity imparts no functional advantage on the CD8+ T cell response to cognate viral peptides. *Proc. Natl. Acad. Sci. USA* 105: 2034–2039.
25. Turner, S. J., G. Diaz, R. Cross, and P. C. Doherty. 2003. Analysis of clonotype distribution and persistence for an influenza virus-specific CD8+ T cell response. *Immunity* 18: 549–559.
26. Venturi, V., K. Kedzierska, M. M. Tanaka, S. J. Turner, P. C. Doherty, and M. P. Davenport. 2008. Method for assessing the similarity between subsets of the T cell receptor repertoire. *J. Immunol. Methods* 329: 67–80.
27. Kalergis, A. M., N. Boucheron, M. A. Doucey, E. Palmieri, E. C. Goyarts, Z. Vegh, I. F. Luescher, and S. G. Nathenson. 2001. Efficient T cell activation requires an optimal dwell-time of interaction between the TCR and the pMHC complex. *Nat. Immunol.* 2: 229–234.
28. Deckhut, A. M., W. Allan, A. McMickle, M. Eichelberger, M. A. Blackman, P. C. Doherty, and D. L. Woodland. 1993. Prominent usage of V beta 8.3 T cells in the H-2Db-restricted response to an influenza A virus nucleoprotein epitope. *J. Immunol.* 151: 2658–2666.
29. Belz, G. T., W. Xie, J. D. Altman, and P. C. Doherty. 2000. A previously unrecognized H-2D(b)-restricted peptide prominent in the primary influenza A virus-specific CD8(+) T-cell response is much less apparent following secondary challenge. *J. Virol.* 74: 3486–3493.
30. Farragher, S. M., A. Tanney, R. D. Kennedy, and D. Paul Harkin. 2008. RNA expression analysis from formalin fixed paraffin embedded tissues. *Histochem. Cell Biol.* 130: 435–445.
31. Kristensen, N. N., A. N. Madsen, A. R. Thomsen, and J. P. Christensen. 2004. Cytokine production by virus-specific CD8(+) T cells varies with activation state and localization, but not with TCR avidity. *J. Gen. Virol.* 85: 1703–1712.
32. Neveu, B., E. Debeaupuis, K. Echasserieau, B. le Moullac-Vaidye, M. Gassin, L. Jegou, J. Decalf, M. Albert, N. Ferry, J. Gournay, et al. 2008. Selection of high-avidity CD8 T cells correlates with control of hepatitis C virus infection. *Hepatology* 48: 713–722.
33. Alexander-Miller, M. A., G. R. Leggatt, and J. A. Berzofsky. 1996. Selective expansion of high- or low-avidity cytotoxic T lymphocytes and efficacy for adoptive immunotherapy. *Proc. Natl. Acad. Sci. USA* 93: 4102–4107.
34. Gallimore, A., T. Dumrese, H. Hengartner, R. M. Zinkernagel, and H. G. Rammensee. 1998. Protective immunity does not correlate with the hierarchy of virus-specific cytotoxic T cell responses to naturally processed peptides. *J. Exp. Med.* 187: 1647–1657.
35. Belyakov, I. M., V. A. Kuznetsov, B. Kelsall, D. Klinman, M. Moniuszko, M. Lemon, P. D. Markham, R. Pal, J. D. Clements, M. G. Lewis, et al. 2006. Impact of vaccine-induced mucosal high-avidity CD8+ CTLs in delay of AIDS viral dissemination from mucosa. *Blood* 107: 3258–3264.
36. Valmori, D., V. Dutoit, V. Schnuriger, A. L. Quiquerez, M. J. Pittet, P. Guillaume, V. Rubio-Godoy, P. R. Walker, D. Rimoldi, D. Liénard, et al. 2002. Vaccination with a Melan-A peptide selects an oligoclonal T cell population with increased functional avidity and tumor reactivity. *J. Immunol.* 168: 4231–4240.
37. Dutoit, V., V. Rubio-Godoy, P. Y. Dietrich, A. L. Quiqueres, V. Schnuriger, D. Rimoldi, D. Liénard, D. Speiser, P. Guillaume, P. Batard, et al. 2001. Heterogeneous T-cell response to MAGE-A10(254-262): high avidity-specific cytolytic T lymphocytes show superior antitumor activity. *Cancer Res.* 61: 5850–5856.
38. Zeh, H. J., III, D. Perry-Lalley, M. E. Dudley, S. A. Rosenberg, and J. C. Yang. 1999. High avidity CTLs for two self-antigens demonstrate superior in vitro and in vivo antitumor efficacy. *J. Immunol.* 162: 989–994.
39. Jenkins, M. R., R. Webby, P. C. Doherty, and S. J. Turner. 2006. Addition of a prominent epitope affects influenza A virus-specific CD8+ T cell immunodominance hierarchies when antigen is limiting. *J. Immunol.* 177: 2917–2925.
40. Pham, N. L., V. P. Badovinac, and J. T. Harty. 2009. A default pathway of memory CD8 T cell differentiation after dendritic cell immunization is deflected by encounter with inflammatory cytokines during antigen-driven proliferation. *J. Immunol.* 183: 2337–2348.
41. Joshi, N. S., W. Cui, A. Chandele, H. K. Lee, D. R. Urso, J. Hagman, L. Gapin, and S. M. Kaech. 2007. Inflammation directs memory precursor and short-lived effector CD8(+) T cell fates via the graded expression of T-bet transcription factor. *Immunity* 27: 281–295.
42. Pipkin, M. E., J. A. Sacks, F. Cruz-Guilloty, M. G. Lichtenheld, M. J. Bevan, and A. Rao. 2010. Interleukin-2 and inflammation induce distinct transcriptional programs that promote the differentiation of effector cytolytic T cells. *Immunity* 32: 79–90.
43. Kalia, V., S. Sarkar, S. Subramaniam, W. N. Haining, K. A. Smith, and R. Ahmed. 2010. Prolonged interleukin-2Ralpha expression on virus-specific CD8+ T cells favors terminal-effector differentiation in vivo. *Immunity* 32: 91–103.